Inorganic Nanoplatforms for Simultaneous Cancer Imaging and Therapy: Status and Challenges

Mian Chen*

Paul C. Lauterbur Research Center for Biomedical Imaging, Institute of Biomedical and Health Engineering, Shenzhen Institutes of Advanced Technology, Chinese Academy of Sciences, Shenzhen 518055, China

Abstract: Functional nanomaterials have inspired revolutionary methods for cancer early diagnosis, treatment, and prevention. For instance, the imaging property of nanomaterials with high resolution and sensitivity can be used for noninvasive detection of cancer and visualization of drug transport. Meanwhile, the therapeutic property of nanomaterials with controllable fashion will increase therapy efficacy and decrease adverse side effect. Thus, compared to traditional treatment approaches, the nanomaterials which combines imaging and therapeutic functionalities, will be more suitable for cancer theranostics. This review introduces several types of inorganic nanoparticles, including silica nanoparticles, upconversion nanoparticles, iron oxide nanoparticles and gold nanoparticles, which can been explored as theranostic nanoplatforms for simultaneous cancer imaging and therapy. We also cover the ongoing challenges of these nanoparticles in clinical applications.

Keywords: Theranostic, inorganic nanomaterials, silica nanoparticles, upconversion nanoparticles, iron oxide nanoparticles, gold nanoparticles.

INTRODUCTION

Cancer is considered to be one primary cause of death in human disease, leading about 8.2 million worldwide casualties in 2012 [1]. After decades' efforts, currently available cancer detection and treatment have made momentous progress, but they still have significant limitations and are distant from ideal one. For instance, with the inconspicuous distinction between tumor and background at the early stage of tumorigenesis, the detection and imaging of cancer by current imaging modalities remains poor, which in turn will require improvements in resolution and sensitivity by using contrast agents. On the other hand, traditional cancer treatments, such as surgery, radiation, chemotherapy or thermotherapy, is still facing big challenge to provide a precise and efficient treatment of cancer. Moreover, most of diagnosis and treatment are just two independent processes in time and space, which will dramatically increase unnecessary clinics process and medical expenses.

With the development of nanotechnology, functional nanomaterials have inspired revolutionary methods for cancer early diagnosis, treatment, and prevention. For example, magnetic nanoparticles can be used as cancer biomarkers for magnetic resonance imaging (MRI) with high resolution and sensitivity [2-4]. Upconversion nanoparticles can be excited by low energy radiation and then emit high-energy photons, which is benefits for fluorescent detection with low auto-fluorescence background and enhanced tissue-penetration depth [5,6]. Mesoporous nanomaterials hold great promise for drug delivery applications, which can protect the entrapped drugs from premature release but efficiently unload at tumor location in a controllable fashion [7-10]. Gold nanoparticles exhibit specific optical properties, such as localized surface plasmon resonance, which causes high temperatures for cancer thermal therapy [11,12]. More importantly, these nanoparticles mentioned above hold the promise of further development as a multifunctional nanoplatform for cancer theranostic, combining the diagnosis and treatment in an integrated process. Compared to traditional treatment approaches, theranostic nanoplatform will be more suitable for cancer management protocols, from first diagnosis until evaluation of treatment effects. This review summarizes the recent developments in the field of theranositcs using different inorganic nanomatirals, including silica nanoparticles, upconversion nanoparticles, iron oxide nanoparticles and gold nanoparticles.

Silica Nanoparticles

Silica nanoparticles (SiNPs) are one type of the most representative and well established inorganic materials, which can be classified as solid SiNPs, core-shell SiNPs and mesoporous SiNPs [13-16]. The Stöber method and reverse microemulsions are the most common methods to synthesize SiNPs [17,18]. Typically, the pure SiNPs have no imaging properties in

*Address correspondence to this author at the Paul C. Lauterbur Research Center for Biomedical Imaging, Institute of Biomedical and Health Engineering, Shenzhen Institutes of Advanced Technology, Chinese Academy of Sciences, Shenzhen 518055, China; Tel: 86-755-86392268; Fax: 86-755-86392299; E-mail: mian.chen@siat.ac.cn

ISSN: 1929-2260 / E-ISSN: 1929-2279/17

most cases. The designing and selection of imaging agents that will be embedded in the SiNPs become particularly important for imaging detection. For example, organic NIR dyes, such as cyanine 5.5, cyanine 7, indocyanine green (ICG), methylene blue and others, have been widely doped into the solid SiNPs for fluorescence imaging [19]. Inorganic imaging agents, such as quantum dots for fluorescence imaging or magnetic nanoparticles for magnetic resonance imaging, also can be encapsulated into the SiNPs [12,13,16]. These imaging agent-doped SiNPs are highly attractive for cancer detection and imaging due to their low toxicity, high loading capacity, enhanced contrast detection, high stability and convenient surface modification as well as multifunctional construction. In addition to imaging properties, recent researches have uncovered numerous interesting in the drug delivery properties by using core-shell SiNPs or mesoporous SiNPs to circumvent the side effect of chemotherapy. The hole inner and porous architecture can be loaded with drug and then capped with various materials as gate-keepers. Under different internal or external stimuli, the loaded drug can be controllable release, which is a very important prerequisite that impacts the therapeutic efficacy and the adverse side effects of drugs.

As SiNPs are excellent scaffolds for simultaneously loading of a wide variety of imaging and therapeutic moieties, they are considered to have great potential for theranostic applications. In 2008, He *et al*. have developed SiNPs-based theranostic for simultaneous *in vivo* imaging and photodynamic therapy by encapsulating methylene blue (MB) alone in the phosphonate-terminated silica matrix [14]. MB is a photosensitizer that can release reactive oxygen species (ROS) under visible light irradiation, resulting in photodamage and subsequent cell death. Meanwhile, MB is also the most inexpensive of the commercially available NIR fluorescent dyes, and has been widely used for bio-analysis. Like other photosensitizers used in clinical applications, MB are no specific that will lead to adverse side effects. In the research, they demonstrated that silica matrix could effectively prevent the leakage of entrapped MB from the particles and provide protection by the phosphonate-terminated for against enzymatic reduction. Thanks to their small size, the SiNPs could accumulate in a tumor because of the well-known enhanced permeability and retention effect (EPR). Then, it was shown that the MB-encapsulated SiNPs could be utilized as a marker under *in vivo* optical imaging system for accurate site-directed irradiation and resulting effective PDT for cancer therapy. Instead of one agent loaded into SiNPs, two different molecule agents such as indocyanine green (ICG) and coralyne alkaloid have also been loaded into poly(A) modified-mesoporous SiNPs for cancer cell theranostic by Chen *et al.* in 2014 [20]. In the system, ICG is not only a famous NIR fluorescence dye approved by the United States Food and Drug Administration (FDA), but also shows high efficiency for converting NIR light into heat, which is fascinating for hyperthermal applications. However, free ICG would bind plasmatic proteins and then be quickly cleared from systemic blood circulation, preventing its further application in clinical cancer treatment. After co-loading of poly(A) modified-mesoporous SiNPs with ICG and coralyne, the pores were capped by the cooperative binding of poly(A) strands through the intercalation of coralyne units into adenosine quadruplex units. Under low-pH or high-temperature conditions, the cooperative binding of poly(A) strands was unstable, leading to the open-gate state. Thus, the system integrated such capabilities as the co-loading of imaging agent and drug cargos, dual pH- and NIR-responsive controlled release, and the combination of chemotherapy and photothermal treatment into one simply constructed platform. Recently, Chen *et al*. have developed a new category of theranostic nanoparticle by using a photothermally sensitive copper sulfide nanoparticles encapsulated in mesoporous silica shells, followed by loading of doxorubicin hydrochloride (DOX) into meso-channels and then multistep surface engineered with amino groups ($-NH_2$), NOTA (1,4,7-triazacyclononane-triacetic acid, a well-known chelator for copper-64 [^{64}Cu] labeling), polyethylene glycol (PEG, for improved *in vivo* biocompatibility and stability), TRC105 (a human/murine chimeric IgG1 monoclonal antibody, which binds to both human and murine CD105 on tumor neovasculature) and finally the radioisotope ^{64}Cu (a positron emitter with a 12.7 h half-life, for positron emission tomography [PET] imaging and biodistribution studies) [21]. As shown in Figure **1**, they demonstrated that this system had a significant potential for a specific and significantly enhanced tumor vasculature detection, targeted photothermally enhanced drug delivery and thermo-chemotherapy. As will be mentioned later, upconversion nanoparticles, iron oxide nanoparticles or gold nanoparticles encapsulated in SiNPs also have been developed for cancer theranostic.

Upconversion Nanoparticles

Upconversion nanoparticles (UCNPs) are rare-earth doped inorganic nanomaterials, mainly containing

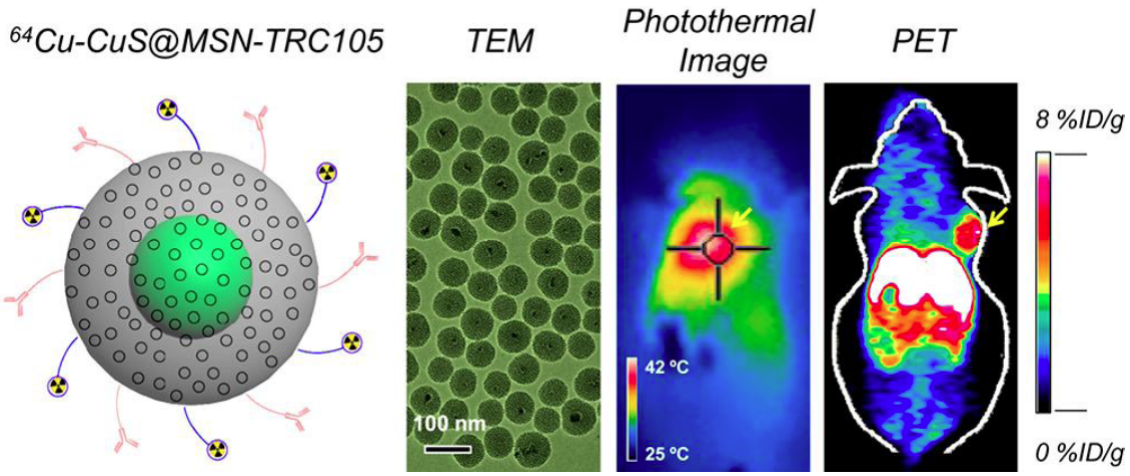

Figure 1: *In vivo* tumor vasculature targeting of CuS@MSN based theranostic nanomedicine. (Reproduced with permission from Ref. [21]. Copyright 2015 American Chemical Society).

ytterbium (Yb), erbium (Er) or thulium (Tm) elements that Yb acts as light absorber (sensitizer) and the Er or Tm acts as emitter (the activator) [22]. Compared with fluorescent agents based on energy down-conversion, UCNPs can be excited by low-energy radiation and then emit high-energy photon [23]. This anti-Stokes mechanism shows various benefits including the significantly reduced auto-fluorescence background, improved tissue penetration depth, and enhanced photostability [24]. In addition, UCNPs can be readily fabricated with various sizes and shapes by well-developed methods, providing an efficient conjugation of targeting ligands or other surface modification [25,26]. For these attractive properties, UCNPs have been widely used as powerful fluorescent nanoprobes for bio-detection and bio-imaging, and many excellent reviews have been published [22,24,26].

Nevertheless, the absolute fluorescence quantum yield of lanthanide-doped core-only UCNPs is low. For example, several hexagonal $NaYF_4$: 2% Er^{3+}, 20% Yb^{3+} NPs with particle sizes ranging from 10 to 100 nm have been reported with quantum yield in the range of 0.005% to 0.3% [27]. These results may be attributed to the increased relative amount of doping ions and surface defects close to the surface of the nanocrystallite [28]. Hence, a range of chemical approaches have been explored to fabricate high quantum yield UCNPs. Developing core-shell UCNPs is an effective solution method, which introduces an inert undoped material as crystalline shell to reduce the non-radiative energy dissipation of UCNPs and improve the luminescence efficiency. For example, Chen *et al*. and Wang *et al*. synthesized the core-shell structured ($NaYbF_4$:Tm^{3+})/CaF_2 NPs, and found that the fluorescence intensity of UCNPs increased about 35 times and 300 times, respectively, comparing to the pristine core NPs [29,30].

As UCNP itself has a specific fluorescent properties, the efforts on the theranostic applications mainly focus on the construction of drug delivery or other therapeutic moieties [31]. For this purpose, several classes of strategies are available:

i) using polymer grafting or self-assembly on the surface of UCNP, and then loading the antitumor drug molecules by physical absorption or covalent association. For example, Jia *et al*. have developed a poly(acrylicacid)-modified $NaYF_4$:Yb/Er UCNP (PAA-UCNP) for simultaneous pH-triggered drug delivery and release imaging [32]. The PAA polymer coated on the surface of UCNP serve as a pH-sensitive shell for loading DOX via electrostatic interaction. By taking advantages of the upconversion fluorescence resonance energy transfer (UFRET) between UCNPs and DOX, the drug release process could be monitored by the changes of fluorescent signal between UCNPs and DOX. As shown in Figure **2**, Ma *et al*. used an amphiphilic tri-block copolymer mPEG-b-PCL-b-PLL conjugated with a cisplatin (IV) prodrug that could be assembled with hydrophobic UCNP to form core-shell structured nanocomposites for cisplatin (IV) delivery and biomedical imaging [33]. Wang *et al*. used PEG grafted amphiphilic polymer to modify UCNP, in which DOX could be loaded in the hydrophobic layer by simple physical adsorption via a supramolecular chemistry approach for intracellular drug delivery [34]. Following the same principle, many other polymers can also be employed, such as PEG phospholipids [35],

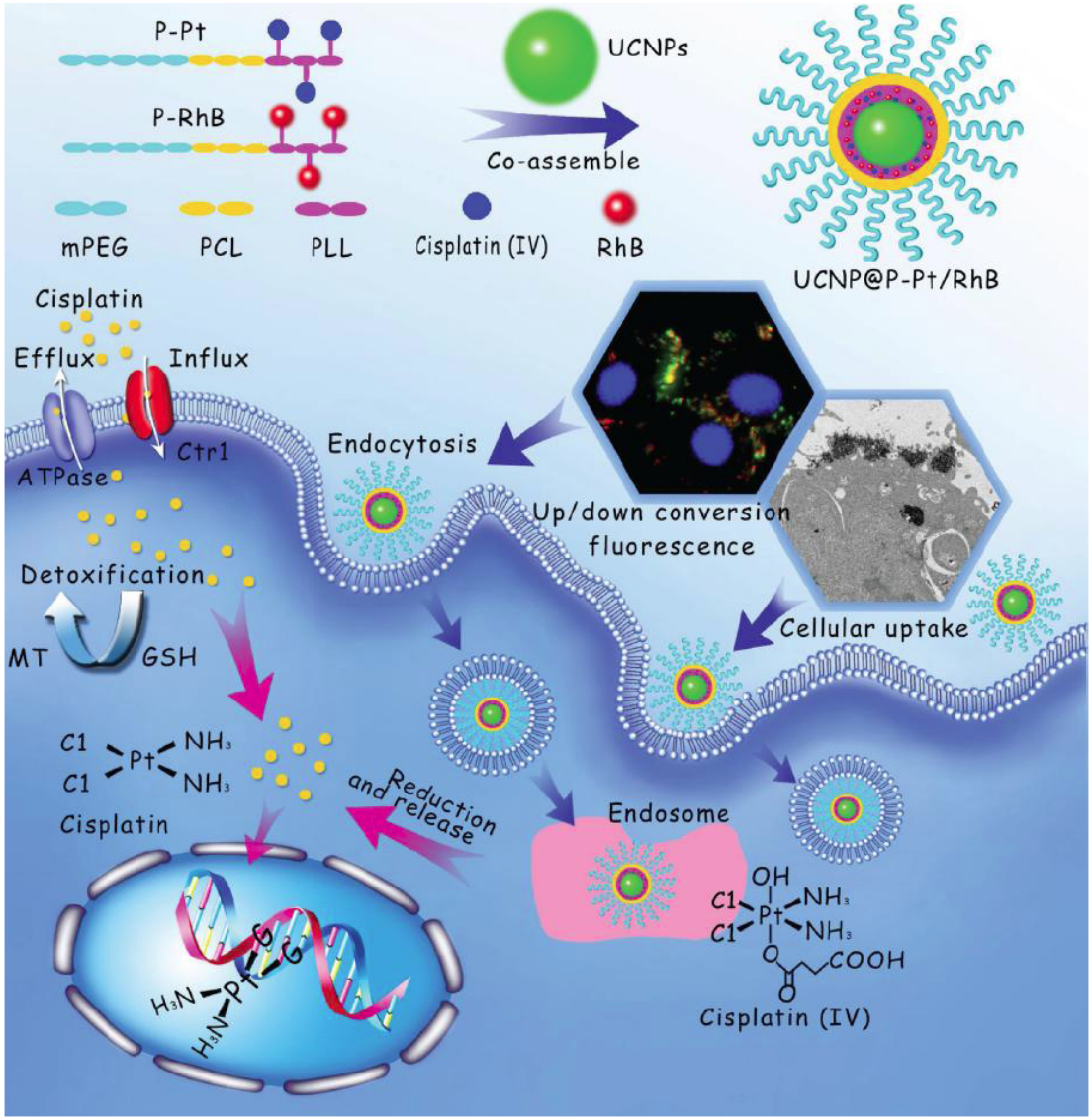

Figure 2: Schematic illustration of the preparation of UCNP@P-Pt/RhB nanoparticles and possible cellular pathways for cisplatin and the nanoparticles UCNP@P-Pt/RhB. (Reproduced with permission from Ref. [33]. Copyright 2013 John Wiley and Sons).

TWEEN [36], PEI [37], BSA [38], poly(styrene-blockallyl alcohol) (PS_{16}-b-PAA_{10}) [39] and so on.

ii) using mesoporous silica or hollow mesoporous silica coating or encapsulation on the surface of UCNPs. These modified UCNPs are chemically stable and much less cytotoxic than the original UCNPs. In addition, the large surface area and pore volume of mesoporous silica ensure facile adsorption as well as high loading of various therapeutic. More importantly, combined with the design of functional moiety as a switch or gate keeper for controlled drug delivery, will offer possibilities of personalized theranostics possible. For example, Dai *et al*. have developed a multifunctional nanocarrier based on thermo/pH-coupling sensitive polymer poly[(N-isopropylacrylamide)-co-(methacrylic acid)] (P(NIPAm-co-MAA)) gated mesoporous silica shell and UCNP core (Figure **3**) [40]. The as-synthesized multifunctional nanocarrier showed bright green up-conversion fluorescence under 980 nm laser excitation and the thermo/pH-sensitive polymer was used as gate keeper to moderate the diffusion of the embedded DOX in-and-out of the pore channels of the silica container. Thus, the system can be used for cancer theranostics, including fluorescence imaging and controlled drug release for therapy. Following the same principle, many other similar studies have been explored and reviewed recently [5].

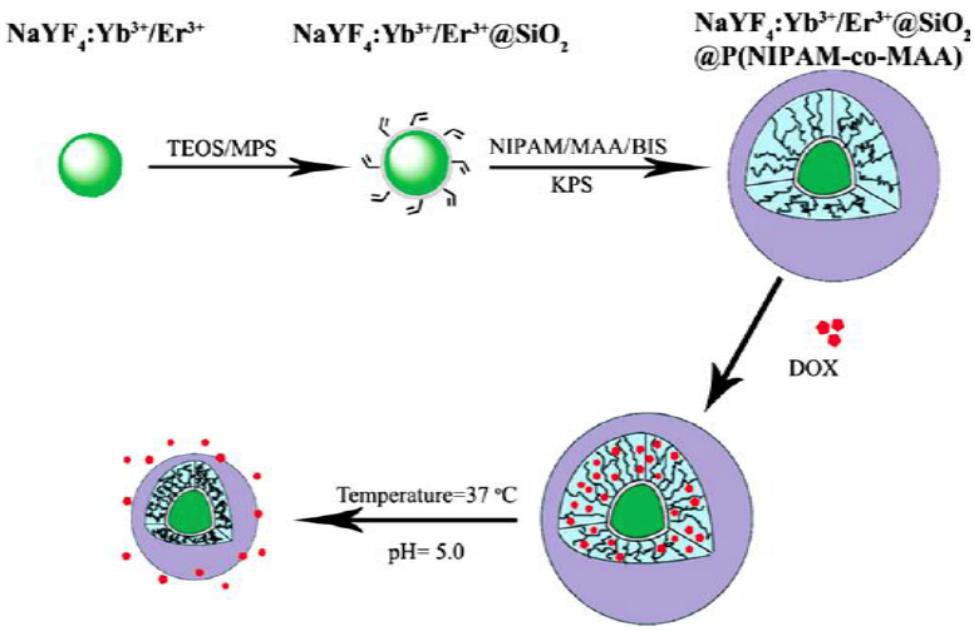

Figure 3: Schematic illustration of the preparation process of $NaYF_4:Yb^{3+}/Er^{3+}$ @SiO_2@P(NIPAM-co-MAA) hybrid microspheres and controlled release of DOX. (Reproduced with permission from Ref. [40]. Copyright 2012 American Chemical Society).

iii) synthesizing hollow UCNPs with a mesoporous surface. For example, Lin`s group have developed different kinds of hollow UCNPs by using uniform $RE(OH)CO_3$ (RE = Gd, Y and Yb) nanospheres as sacrificial templates, which can be further used in drug delivery [41,42].

In addition to the strategies discussed above, some other methods have been developed mainly for simultaneous cancer multimodal imaging and therapy. For example, Liu *et al*. recently used Mn-complex and polydopamine modified core-shell nanocomposites for tri-mode upconversion luminescence (UCL) imaging and T_1-,T_2-weighted MRI guided photothermal therapy [43]. Dai *et al*. also have successfully achieved UCL/MRI/CT tri-modality imaging and NIR-activated platinum pro-drug delivery for photodynamic therapy by using UCNPs with platinum(IV) pro-drug conjugated on the surface (Figure **4**) [44].

Iron Oxide Nanoparticles

Iron oxide nanoparticles (IONPs) are one type of the most widely used magnetic nanoparticles. On the basis of transverse (T_2) relax-ations, iron oxide nanoparticles have already proved their role as contrast agents in MR imaging with excellent anatomic detail, enhanced soft tissue contrast, and high spatial resolution. Meanwhile, because of Neel fluctuation and the energy losses, the IONPs can act as an energy-transfer mediator by transforming an external magnetic field to heat for cancer thermal therapy [45]. For example, Panyam *et al*. have developed EGFR-targeting IONPs for the magnetic hyperthermia treatment of non-small cell lung cancer [46]. Moreover, the IONPs can be delivered more selectively to the target site under the guidance of an external magnetic field [47]. This remote and noninvasive control of iron oxide nanoparticles is very promising because biological tissues are inherently transparent to magnetic fields. However, due to the drag forces associated with blood flow, successful *in vivo* magnetic delivery still has great challenges. Finally, to get additional properties and benefits for cancer theranostic, the optimization of the IONPs surface along with other agents is necessary, such as PEGylation for improving the bio-distribution and bio-compatibility [48], biologically active targeting ligands modification for selective delivery [49], organic or inorganic shell layers for therapeutic agents binding or loading [50], and so on. Thus, IONPs can integrate such capabilities as MR enhancement imaging, magnetic hyperthermia treatment, magnetic targeted delivery as well as multimodal imaging and treatment into one platform for cancer theranostic. For example, Roy *et al*. have prepared a pH and temperature stimuli-responsive polymer modified gadolinium doped iron oxide nanoparticle (poly@Gd-MNPs) for cancer theranostic [51]. Recently, Hu *et al*. synthesized a new multifunctional polycationic Au nanorod-coated Fe_3O_4 nanosphere hierarchical nanocomposite [52]. As shown in Figure **5**, the surface of Fe_3O_4 can combine with polydopamine (PDA) layer by strong electrostatic adsorption, producing negatively charged Fe_3O_4

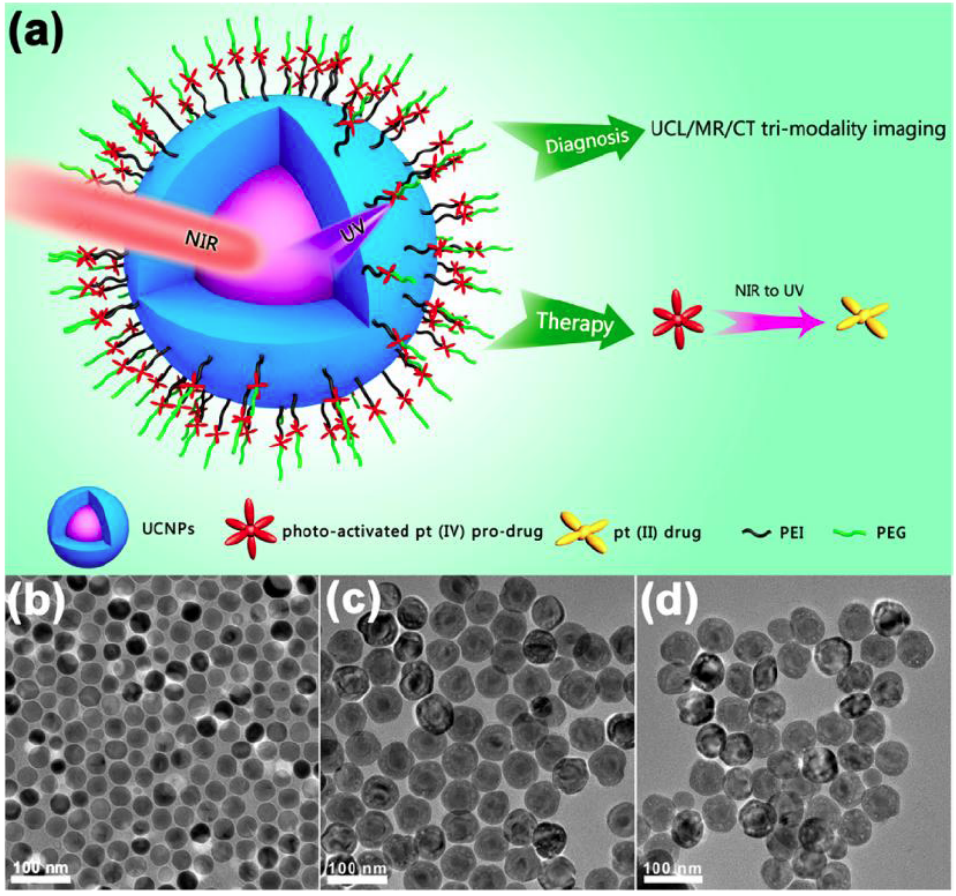

Figure 4: Schematic illustration of the characterization of UCNP-DPP-PEG nanoparticles (**a**). TEM images of oleic-acid-capped $NaYF_4$:Yb^{3+}/Tm^{3+} nanoparticles (**b**), core-shell structured $NaYF_4$:Yb^{3+}/Tm^{3+}@$NaGdF_4$:Yb^{3+} nanoparticles (**c**), and UCNP-DPP-PEG nanoparticles (**d**). (Reproduced with permission from Ref. [44]. Copyright 2013 American Chemical Society).

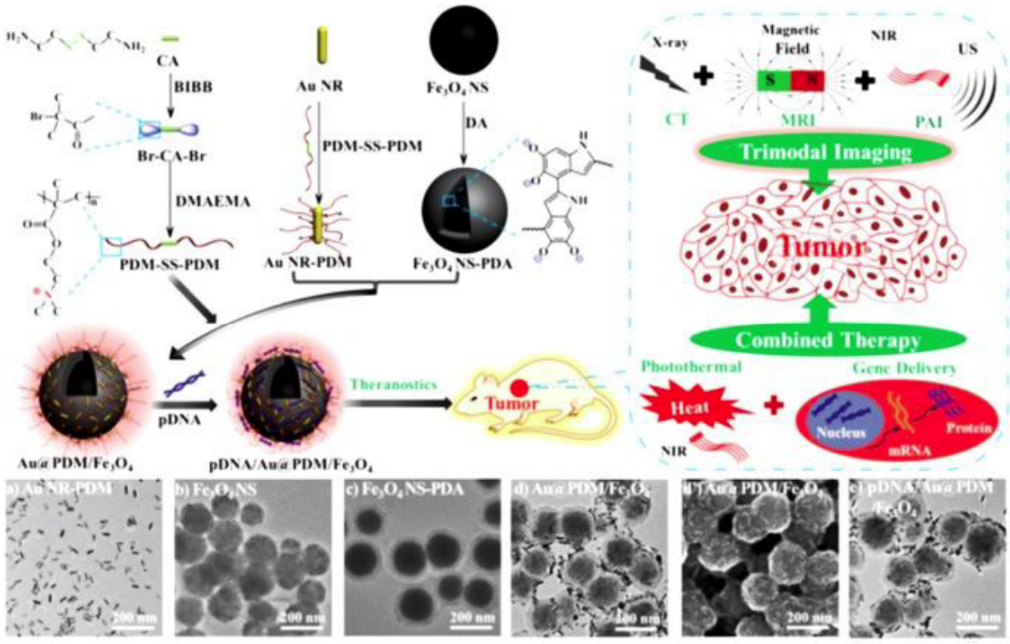

Figure 5: Schematic illustration of the preparation of pDNA/Au@PDM/Fe_3O_4 nanocomposites and their applications for *in vivo* trimodal imaging and combined photothermal/gene therapy. Insets: TEM images of **a**) Au NR-PDM, **b**) Fe_3O_4 NS, **c**) Fe_3O_4 NS-PDA, **d**) Au@PDM/Fe_3O_4, and **e**) pDNA/Au@PDM/Fe_3O_4 (w/w = 30) and SEM image of **d'**) Au@PDM/Fe_3O_4. (Reproduced with permission from Ref. [52]. Copyright 2016 John Wiley and Sons).

NS-PDA. Then, a type of disulfide-linked poly(2-dimethyl amino)ethyl methacrylate (PDM-SS-PDM) was synthesized and introduced onto the Au nanorod surface via its interaction with disulfide bonds, producing positively charged and stabile Au NR-polycation conjugates (Au NR-PDM). Subsequently, the negatively charged Fe_3O_4 NS-PDA core was coated with positively charged Au NR-PDM and PDM-SS-PDM through a consecutive electrostatic assembly, resulting in a ternary Au@PDM/Fe_3O_4 hierarchical nanocomposite. For such nanocomposites, the combined near-infrared absorbance properties of Fe_3O_4-PDA and Au NR-PDM are applied to photoacoustic imaging and photothermal therapy. Besides, Fe_3O_4 and Au NR components allow the nanocomposites to serve as MRI and CT contrast agents. The prepared positively charged Au@PDM/Fe_3O_4 also can complex plasmid DNA into pDNA/Au@pDM/ Fe_3O_4 and efficiently mediated gene therapy. Finally, the developed system could simultaneously realize multimodal imaging of photoaccoustic imaging PAI, CT and MRI and combination of PTT and gene therapy in a xenografted rat glioma (C6) nude mouse model.

In addition to polymer coating, the mesoporous silica modified on the surface of IONPs have also been used to improve their colloidal stability, increase their water-dispersibility, and provide a promising candidate for drug delivery with minimal side-effects. As shown in Figure **6**, a multifunctional theranostic platform based on mesoporous silica-Fe_3O_4 shell-core nanoparticles (MMSNs) was ingeniously designed for tumor-targeted magnetic resonance imaging and precise therapy by Chen *et al*. [53]. Multifunctional molecular machine constructed by platinum(IV) prodrug, β-cyclodextrin (β-CD), and cancer-targeted peptide adamantane-PEG_8-glycine-arginine-glycineaspartic- serine (AD-PEG_8-GRGDS) progressively was anchored on the surface of MMSNs. In the system, Fe_3O_4 core was employed as MRI contrast agent and magnetic enhanced accumulation. The porous structure of the mesoporous silica shell was use for anticancer drug DOX loading. The β -CD was used as the gatekeeper and

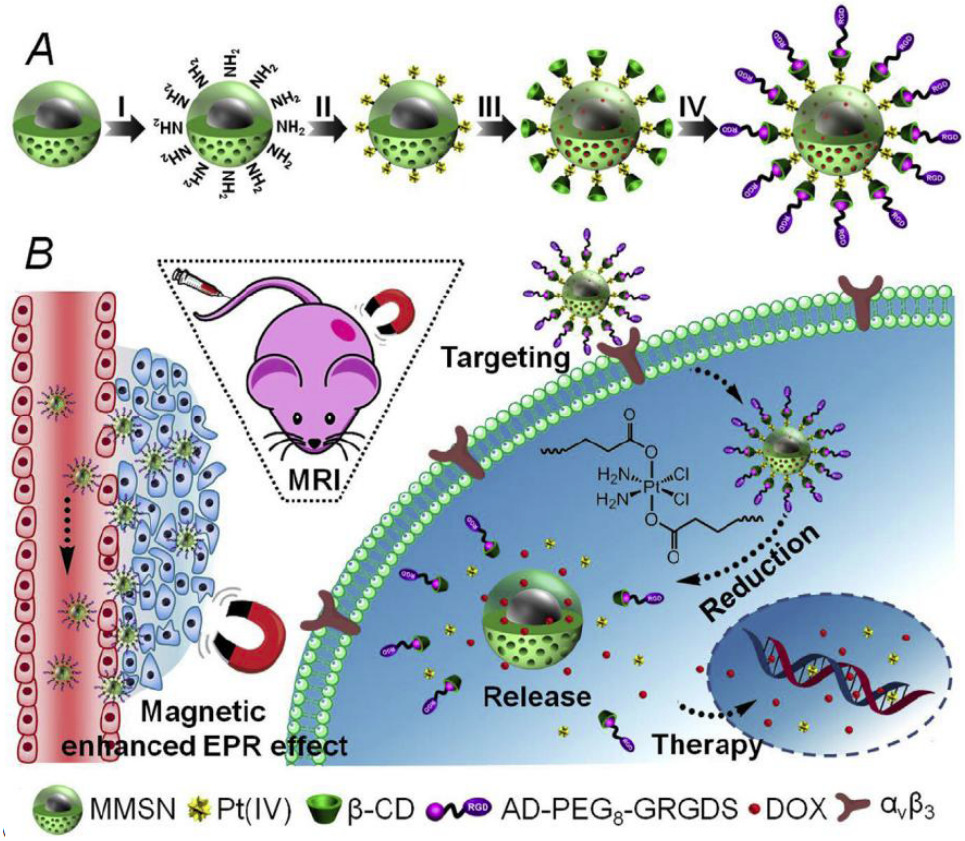

Figure 6: Schematic illustration of the design and proposed mechanism of the multifunctional MMSNs for tumor-targeted MRI and precise therapy. (**A**) The functionalization protocol of the MMSN. (**B**) The precise treatment strategy by using multifunctional MMSNs. Specifically, the magnetic enhanced EPR effect and the active targeting effect facilitated the enriching of MMSNs in tumor sites; then MMSNs were selectively uptaken by cancer cells via the receptor-mediated endocytosis; afterward the platinum(IV) prodrug was reduced by the cellular innate reductive environment and induced the removal of gatekeeper, thereby triggering the in situ drug release for precise therapy. (Reproduced with permission from Ref. [53]. Copyright 2016 Elsevier).

immobilized onto mesoporous silica shell via the linker of platinum(IV) prodrug, which was redox-sensitive and could be intracellularly activated by reduction to the toxic platinum(II) drug. The peptide AD-PEG_8-GRGDS was used as a targeting ligand. After intravenous injection, this multifunctional MMSNs exhibited high contrast in MRI for locating tumor *in vivo* and achieved significant antitumor efficacy with minimal side effects.

With the same principle, Yang *et al*. have developed a theranostic nanoplatform by WS2 nanosheets with their surface pre-adsorbed with IONPs via self-assembly coated with a mesoporous silica shell, on to which polyethylene glycol (PEG) is attached [54]. The obtained multifunctional nanoparticles exhibit many interesting inherent physical properties, including high near-infrared light and X-ray absorbance, strong superparamagnetism, NIR-induced drug controlled release, as well as three-modal imaging (fluorescence, MRI, and X-ray computed tomography imaging) and two-modal treatment (photothermal and chemotherapy).

Gold Nanoparticles

Gold nanoparticles (AuNPs), as one of the most important inorganic nanopraticles, have attracted much attention owing to their unique feature [55]. Firstly, with strong and tunable surface plasmon resonance (SPR) properties throughout the near-infrared region, many kind of AuNPs including gold nanorods, gold nanocages, gold nanostars and gold nanoshells can be used as photoacoustic contrast agents for cancer imaging with high spatial resolution and a deeper imaging depth [56,57]. In addition, with a high efficiency for the conversion of the NIR light into heat, these gold nanostructures provide the fundamental basis of the hyperthermal cancer therapy [58]. More interestingly, with the unique structures of AuNPs (such as gold nanocages) or surface functional design (such as polymer, biomacromolecule or mesoporous silica shell modification), the AuNPs can be explored as drug carriers for drug controlled release with low side-effects [59]. Finally, the straightforward synthesis and biocompatibility and easy surface modification are additional advantages for fabricating AuNPs as a promising theranostic nanoplatform for simultaneous cancer imaging and therapy [60,61]. For example, Kim *et al*. have used gold nanocages for *in vivo* molecular photoacoustic tomography of melanomas [62]. The results showed that the injection dosage of gold nanocages was much lower than that of single walled carbon nanotubes or gold nanorods for cancer sensitivity detection. Xia *et al*. have constructed a series of gold nanocages based nanocarriers for photothermal treatment and drug delivery [63]. Srivatsan *et al*. recently used poly(ethylene glycol) modified gold nanocages to noncovalently entrap a photosensitizer for *in vivo* tumor photoacoustic image and therapy simultaneously [64]. They demonstrated that the therapeutic efficacy using AuNPs was superior to the free drug. As shown in Figure **7**, Huang *et al*. have developed a photo-theranostic agent based on chlorin e6 photosensitizer-conjugated silica-coated gold

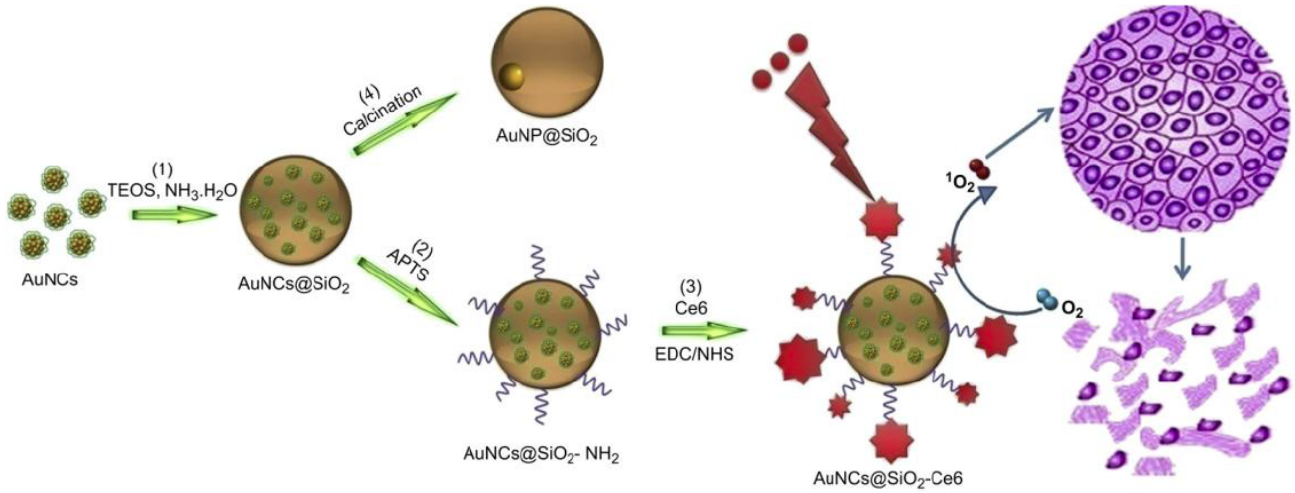

Figure 7: Illustration of the synthetic procedure of Ce6-conjugated silica-coated gold nanoclusters (AuNCs@SiO_2-Ce6) for photodynamic therapy and the calcination of AuNCs@SiO_2 into AuNP@SiO2. (1) AuNCs were coated by a silica layer to form a fluorescent coreeshell nanostructure using a modified Stöber method. (2) A silane coupling agent, 3-aminopropyltrimethoxysilane (APTS), was used to modify the silica surface for further conjugation. (3) Covalent binding of Ce6 to the AuNCs@SiO_2-NH_2 was performed using a modified EDC-NHS reaction. (4) AuNCs@SiO_2 was calcined at 600 ^{o}C for 2 h to fuse into GNP@SiO_2. (Reproduced with permission from Ref. [65]. Copyright 2013 Elsevier).

nanoclusters, which can be used for fluorescence imaging-guided photodynamic therapy [65]. Recently, Sun *et al*. integrated ^{64}Cu to a variety of PEG-stabilized AuNPs of different sizes and shapes via chemical reduction of $^{64}CuCl_2$ under mild reaction conditions for positron emission tomography (PET) imaging12. They also integrated ^{64}Cu onto arginine-glycine-aspartic acid (RGD) peptide modified gold nanorods for PET image-guided photothermal therapy. Liu *et al*. developed a surfactant-free gold nanostar probe for multi-modality theranostics including surface-enhanced Raman scattering (SERS) detection, x-ray computed tomography, two-photon luminescence imaging, and photothermal therapy [66]. Song *et al*. reported a hybrid reduced graphene oxide (rGO)-loaded ultrasmall plasmonic gold nanorod vesicle (rGO-AuNRVe) with remarkably amplified photoacoustic performance and photothermal effects [67]. Meanwhile, DOX and DOX-loaded rGO could both be encapsulated into the hybrid vesicle, resulting in a dual photo- and acid-responsive DOX release pattern, useful for a remote-controlled drug release.

CONCLUSIONS AND CHALLENGES

The application of inorganic nanoplatforms for simultaneous cancer imaging and therapy has attracted outstanding attention in recent years. With excellent imaging and therapeutic properties, inorganic nanoplatforms not only provide promising various imaging modalities including optical imaging, photoacoustic imaging, MRI, CT and PET imaging, but also provide various therapeutic modalities including chemotherapy, thermotherapy, photodynamic, combination therapy, and drug delivery with more controllable fashion. Thus, there are many strategies that can combine imaging and therapy for optimizing the theranostic regimes. Here we only discuss platforms related to silica nanoparticles, upconversion nanoparticles, iron oxide nanoparticles and gold nanoparticles as examples to illustrate the potential of inorganic nanoparticle for cancer theranostics. By the combination of imaging and therapy function, these nanocomposites provide more accurate intervention to identify the location of tumor, monitor the distribution and location of nanocomposites, and assess the therapeutic outcome in real time. However, although the development of inorganic nanoplatforms for simultaneous cancer imaging and therapy have been directed to the development of cancer personalized theranostic, most of systems are just in concept of proof stage and far from utilization in a clinical setting. There still face significant challenges to overcome before we can ensure successful translation of these concepts to the clinic. First, many nanocomposites with multifunctional construction suffer from tedious and rigorous synthesis process, leading to difficult to reproduce or large-scale manufacture. Second, as imaging and therapy have different requirements for equipment, there are lack of highly integrated medical equipment for theranostic operation, leading to insufficient relationships between imaging results and therapeutic efficacy in time and space. Third, the potential cytotoxicity and the information on absorption, distribution, metabolism and excretion of the nanocomposites should be paid more attention, especially as a variety of nanoparticles have been reported to induce cytotoxicity, genotoxicity, and immunotoxicity related to their nanometer size, treatment dose or components. While still in an early phase of development, we believe inorganic nanoplatforms for simultaneous cancer imaging and therapy will have significant impact on improving cancer care in the near future.

ACKNOWLEDGEMENTS

This work was supported in part by the National Natural Science Foundation of China (Grant Nos. 21505149), China Postdoc-toral Science Foundation (Grant No. 2015M582438).

REFERENCES

[1] Available from: http://www.who.int/cancer/en/

[2] Sun C, Lee JS, Zhang M. Adv Drug Deliv Rev 2008; 60: 1252-1265. http://dx.doi.org/10.1016/j.addr.2008.03.018

[3] Lee N, Yoo D, Ling D, Cho MH, Hyeon T, Cheon J. Chem Rev 2015; 115: 10637-10689. http://dx.doi.org/10.1021/acs.chemrev.5b00112

[4] Bauer LM, Situ SF, Griswold MA, Samia ACS. J Phys Chem Lett 2015; 6: 2509-2517. http://dx.doi.org/10.1021/acs.jpclett.5b00610

[5] Liu JN, Bu WB, Shi JL. Acc Chem Res 2015; 48: 1797-1805. http://dx.doi.org/10.1021/acs.accounts.5b00078

[6] Tsang MK, Bai G, Hao J. Chem Soc Rev 2015; 44: 1585-1607. http://dx.doi.org/10.1039/C4CS00171K

[7] Vivero-Escoto JL, Huxford-Phillips RC, Lin W. Chem Soc Rev 2012; 41: 2673-2685. http://dx.doi.org/10.1039/c2cs15229k

[8] Slowing II, Vivero-Escoto JL, Wu CW, Lin VSY. Adv Drug Deliv Rev 2008; 60: 1278-1288. http://dx.doi.org/10.1016/j.addr.2008.03.012

[9] Ciriminna R, Fidalgo A, Pandarus V, Béland F, Ilharco LM, Pagliaro M. Chem Rev 2013; 113: 6592-6620. http://dx.doi.org/10.1021/cr300399c

[10] Wang Y, Zhao Q, Han N, *et al*. Nanomedicine 2015; 11: 313-327.

[11] Xia Y, Li W, Cobley CM, *et al*. Acc Chem Res 2011; 44: 914-924. http://dx.doi.org/10.1021/ar200061q

[12] Kodiha M, Wang YM, Hutter E, Maysinger D, Stochaj U. Theranostics 2015; 5: 357-370. http://dx.doi.org/10.7150/thno.10657

[13] Ow H, Larson DR, Srivastava M, Baird BA, Webb WW, Wiesner U. Nano Lett 2005; 5: 113-117. http://dx.doi.org/10.1021/nl0482478

[14] He X, Wu X, Wang K, Shi B, Hai L. Biomaterials 2009; 30: 5601-5609. http://dx.doi.org/10.1016/j.biomaterials.2009.06.030

[15] Slowing II, Trewyn BG, Giri S, Lin VY. Adv Funct Mater 2007; 17: 1225-1236. http://dx.doi.org/10.1002/adfm.200601191

[16] Cauda V, Schlossbauer A, Kecht J, Zürner A, Bein T. J Am Chem Soc 2009; 131: 11361-11370. http://dx.doi.org/10.1021/ja809346n

[17] Rossi LM, Shi L, Quina FH, Rosenzweig Z. Langmuir 2005; 21: 4277-4280. http://dx.doi.org/10.1021/la0504098

[18] Zhao X, Bagwe RP, Tan W. Adv Mater 2004; 16: 173-176. http://dx.doi.org/10.1002/adma.200305622

[19] He X, Wang K, Cheng Z. Wiley Interdiscip Rev Nanomed Nanobiotechnol 2010; 2: 349-366. http://dx.doi.org/10.1002/wnan.85

[20] Chen M, Yang S, He X, Wang K, Qiu P, He D. J Mater Chem B 2014; 2: 6064-6071. http://dx.doi.org/10.1039/C4TB01040J

[21] Chen F, Hong H, Goel S, *et al*. ACS Nano 2015; 9: 3926-3934. http://dx.doi.org/10.1021/nn507241v

[22] Wang F, Liu X. Chem Soc Rev 2009; 38: 976-989. http://dx.doi.org/10.1039/b809132n

[23] Feng W, Han C, Li F. Adv Mater 2013; 25: 5287-5303. http://dx.doi.org/10.1002/adma.201301946

[24] Yao C, Tong Y. Trends Analyt Chem 2012; 39: 60-71. http://dx.doi.org/10.1016/j.trac.2012.07.007

[25] Ye X, Collins JE, Kang Y, *et al*. Proc Natl Acad Sci U S A 2010; 107: 22430-22435. http://dx.doi.org/10.1073/pnas.1008958107

[26] Liu Y, Tu D, Zhu H, Chen X. Chem Soc Rev 2013; 42: 6924-6958. http://dx.doi.org/10.1039/c3cs60060b

[27] Boyer JC, Van Veggel FC. Nanoscale 2010; 2: 1417-1419. http://dx.doi.org/10.1039/c0nr00253d

[28] Gnach A, Bednarkiewicz A. Nano Today 2012; 7: 532-563. http://dx.doi.org/10.1016/j.nantod.2012.10.006

[29] Chen G, Shen J, Ohulchanskyy TY, *et al*. ACS Nano 2012; 6: 8280-8287. http://dx.doi.org/10.1021/nn302972r

[30] Wang YF, Sun LD, Xiao JW, *et al*. Chem Eur J 2012; 18: 5558-5564. http://dx.doi.org/10.1002/chem.201103485

[31] Yang D, Hou Z, Cheng Z, Li C, Lin J. Chem Soc Rev 2015; 44: 1416-1448. http://dx.doi.org/10.1039/C4CS00155A

[32] Jia X, Yin J, He D, *et al*. J Biomed Nanotechnol 2013; 9: 2063-2072. http://dx.doi.org/10.1166/jbn.2013.1764

[33] Ma PA, Xiao H, Li X, *et al*. Adv Mater 2013; 25: 4898-4905. http://dx.doi.org/10.1002/adma.201301713

[34] Wang C, Cheng L, Liu Z. Biomaterials 2011; 32: 1110-1120. http://dx.doi.org/10.1016/j.biomaterials.2010.09.069

[35] Tian G, Gu Z, Zhou L, *et al*. Adv Mater 2012; 24: 1226-1231. http://dx.doi.org/10.1002/adma.201104741

[36] Tian G, Yin W, Jin J, *et al*. J Mater Chem B 2014; 2: 1379-1389. http://dx.doi.org/10.1039/c3tb21394c

[37] Wang F, Chatterjee DK, Li Z, Zhang Y, Fan X, Wang M. Nanotechnology 2006; 17: 5786-5791. http://dx.doi.org/10.1088/0957-4484/17/23/013

[38] Chen Q, Wang C, Cheng L, He W, Cheng Z, Liu Z. Biomaterials 2014; 35: 2915-2923. http://dx.doi.org/10.1016/j.biomaterials.2013.12.046

[39] Xu H, Cheng L, Wang C, Ma X, Li Y, Liu Z. Biomaterials 2011; 32: 9364-9373. http://dx.doi.org/10.1016/j.biomaterials.2011.08.053

[40] Dai Y, Ma PA, Cheng Z, *et al*. ACS Nano 2012; 6: 3327-3338. http://dx.doi.org/10.1021/nn300303q

[41] Kang X, Yang D, Dai Y, *et al*. Nanoscale 2013; 5: 253-261. http://dx.doi.org/10.1039/C2NR33130F

[42] Yang D, Kang X, Dai Y, Hou Z, Cheng Z, Li C, Lin J. Biomaterials 2013; 34: 1601-1612. http://dx.doi.org/10.1016/j.biomaterials.2012.11.004

[43] Liu T, Li S, Liu Y, Guo Q, Wang L, Liu D, Zhou J. J Mater Chem B 2016; 4: 2697-2705. http://dx.doi.org/10.1039/C5TB02785C

[44] Dai Y, Xiao H, Liu J, *et al*. J Chem Soc Rev 2013; 135: 18920-18929. http://dx.doi.org/10.1021/ja410028q

[45] Hilger I, Hiergeist R, Hergt R, Winnefeld K, Schubert H, Kaiser WA. Invest Radiol 2002; 37: 580-586. http://dx.doi.org/10.1097/00004424-200210000-00008

[46] Sadhukha T, Wiedmann TS, Panyam J. Biomaterials 2013; 34: 5163-5171. http://dx.doi.org/10.1016/j.biomaterials.2013.03.061

[47] Cole AJ, David AE, Wang J, Galbán CJ, Hill HL, Yang VC. Biomaterials 2011; 32: 2183-2193. http://dx.doi.org/10.1016/j.biomaterials.2010.11.040

[48] Liu D, Wu W, Ling J, Wen S, Gu N, Zhang X. Adv Funct Mater 2011; 21: 1498-1504. http://dx.doi.org/10.1002/adfm.201001658

[49] Schleich N, Po C, Jacobs D, *et al*. J Control Release 2014; 194: 82-91. http://dx.doi.org/10.1016/j.jconrel.2014.07.059

[50] Zhao W, Gu J, Zhang L, Chen H, Shi J. J Am Chem Soc 2005; 127: 8916-8917. http://dx.doi.org/10.1021/ja051113r

[51] Roy E, Patra S, Madhuri R, Sharma PK. Colloids Surf B Biointerfaces 2016; 142: 248-258. http://dx.doi.org/10.1016/j.colsurfb.2016.02.053

[52] Hu Y, Zhou Y, Zhao N, Liu F, Xu FJ. Small 2016; 12: 2459-2468. http://dx.doi.org/10.1002/smll.201600271

[53] Chen WH, Luo GF, Lei Q, *et al*. Biomaterials 2016; 76: 87-101. http://dx.doi.org/10.1016/j.biomaterials.2015.10.053

[54] Yang G, Gong H, Liu T, Sun X, Cheng L, Liu Z. Biomaterials 2015; 60: 62-71. http://dx.doi.org/10.1016/j.biomaterials.2015.04.053

[55] Daniel MC, Astruc D. Chem Rev 2004; 104: 293-346. http://dx.doi.org/10.1021/cr030698+

[56] Nie L, Wang S, Wang X, *et al*. Small 2014; 10: 1585-1593. http://dx.doi.org/10.1002/smll.201302924

[57] Li W, Chen X. Nanomedicine 2015; 10: 299-320. http://dx.doi.org/10.2217/nnm.14.169

[58] Kennedy LC, Bickford LR, Lewinski NA, *et al*. Small 2011; 7: 169-183. http://dx.doi.org/10.1002/smll.201000134

[59] Yavuz MS, Cheng Y, Chen J, *et al*. Nat Mater 2009; 8: 935-939. http://dx.doi.org/10.1038/nmat2564

[60] Moon GD, Choi SW, Cai X, *et al*. J Am Chem Soc 2011; 133: 4762-4765. http://dx.doi.org/10.1021/ja200894u

[61] Huang P, Rong P, Lin J, *et al*. J Am Chem Soc 2014; 136: 8307-8313. http://dx.doi.org/10.1021/ja503115n

[62] Kim C, Cho EC, Chen J, *et al*. ACS Nano 2010; 4: 4559-4564. http://dx.doi.org/10.1021/nn100736c

[63] Skrabalak SE, Chen J, Sun Y, *et al*. Acc Chem Res 2008; 41: 1587-1595. http://dx.doi.org/10.1021/ar800018v

[64] Srivatsan A, Jenkins SV, Jeon M, *et al*. Theranostics 2014; 4: 163-174. http://dx.doi.org/10.7150/thno.7064

[65] Huang P, Lin J, Wang S, *et al*. Biomaterials 2013; 34: 4643-4654. http://dx.doi.org/10.1016/j.biomaterials.2013.02.063

[66] Liu Y, Ashton JR, Moding EJ, *et al*. Theranostics 2015; 5: 946-960. http://dx.doi.org/10.7150/thno.11974

[67] Song J, Yang X, Jacobson O, *et al*. ACS Nano 2015; 9: 9199-9209. http://dx.doi.org/10.1021/acsnano.5b03804

Received on 12-04-2016 Accepted on 03-08-2016 Published on 16-02-2017

DOI: https://doi.org/10.6000/1929-2279.2017.06.01.1